11

# Hydrodynamic Forces on a Circular Cylinder Placed in Wave-Current Co-existing Fields

By

Yuichi IWAGAKI*, Toshiyuki ASANO* and Fumihiro NAGAI**

## Abstract

The in-line hydrodynamic force acting on a circular cylinder in a wave-current co-existing field and its generating mechanism are discussed. This study focuses on the asymmetries of both the water particle movement and the resultant vortex property with respect to the cylinder as being the causes of an inherent generating mechanism of the hydrodynamic force in the wave-current co-existing field.

First of all, the vortex property around a circular cylinder in the wave-adverse current co-existing field is examined by flow visualization tests. It is found that the vortex property depends on the flow characteristics around the trough phase when the wave-current composite velocity becomes maximum and can be represented with a newly proposed $K.C.$ number for the co-existing field.

Next, the characteristics of the in-line force are made clear by evaluating the drag coefficient and the mass coefficient in the expanded Morison's equation for the co-existing field. These coefficients can be well arranged by $(K.C.)_2{}^*$, which is one of the newly proposed $K.C.$ numbers, and their characteristics coincide with the existing results in the wave-only field. The in-line hydrodynamic force in the co-existing field can be explained sufficiently by considering the vortex property in the same manner as clarified in the wave-only field.

## 1. Introduction

Evaluation of wave forces acting on a circular cylinder is one of the most important subjects in coastal and ocean engineering. Recently, Sarpkaya and Isaacson[1] systematically assembled and organized comprehensive research efforts in this field, and they pointed out several problems which remain unsolved. The study on hydrodynamic forces in wave-current co-existing fields is one of such problems. However, research on this subject is scarce and as yet there is not a sufficient understanding. The wave-current co-existing field can be easily obtained either by oscillating a cylinder in the in-line direction in a uniform flow, or by moving it at a constant speed in a harmonically oscillating flow. Verley and Moe[2] examined

\* Department of Civil Engineering, Kyoto University
\*\* Present address, Osaka Municipal Office, Bureau of Civil Engineering, Osaka, 530, Japan

the drag and the mass coefficients by using the former field, while Horikawa et al.[3],[4] treated them in the latter field. However, the existing studies have not sufficiently discussed the hydrodynamic forces based on the vortex properties around a cylinder.

As an essential difference of the generation mechanism of hydrodynamic forces in the wave-current co-existing field from that in the wave-only field, this study focuses on the asymmetry of a water particle movement with respect to a cylinder. In the wave-only field, the water particle moves almost symmetrically in the phases of wave crest and wave trough, whereas in the co-existing field it does asymmetrically due to a superimposed current. Consequently, the properties of the vortex formation, development and shedding become different in the wave-only field, and they produce inherent characteristics in the hydrodynamic forces. From the above mentioned viewpoint, in this study first of all, flow visualization tests are performed in wave and adverse current co-existing fields to examine the vortex properties. Next, the characteristics of the in-line forces are made clear through the experimental data of the drag and the mass coefficients in the expanded Morison's equation to the co-existing field. Finally, the generation mechanism of the hydrodynamic forces associated with the vortex properties is discussed in detail.

## 2. Vortex properties around a circular cylinder in co-existing fields

### (1) Flow visualization test

Experiments were carried out in a wave tank, 27 m long, 0.5 m wide and 0.7 m high, in which a circulating flow can be generated by a power pump. The water depth was kept constant at 30 cm. The vertical circular cylinders used in this test were 30 mm and 60 mm in diameter. Test runs were conducted under conditions that the wave frequency $f$ was 0.5 Hz, the wave heights $H$ were 1.1~3.9 cm, the currents were in the opposite direction to the wave propagation and their velocities varied 0~13.9 cm/sec. The flow visualization around a cylinder was performed with aluminum powder, and photographs of fluid motion at the water surface were taken with a motor-drive camera at the speed of 3 flame per second.

### (2) Classification of vortex patterns in wave-only field

Before examining the vortex patterns in the co-existing field, it is worthwhile to arrange the existing results in the wave-only field. The results on classifications of vortex patterns investigated by Iwagaki-Ishida[5], Sawaragi-Nakamura[6] and Sawamoto-Kikuchi[7] are shown in Table 1. In the former two studies a vertical circular cylinder was used in progressive waves. On the other hand, Sawamoto et al. examined the vortex patterns with a horizontal circular cylinder placed at the node of standing waves. Iwagaki-Ishida classified the vortex patterns not only by the Keulegan-Carpenter number (K.C. in abbreviation) but also by Reynolds

Table 1. Classification of vortex pattern in wave-only field

| Vortex pattern | outline | Sawaragi-Nakamura[6] | Iwagaki-Ishida[5] | Sawamoto-Kikuchi[7] |
|---|---|---|---|---|
| V-1 | No vortex generation | $K.C.<3$ | $K.C.<2$ No separation and No vortex<br><br>$2<K.C.<5$ $Re>2000$ Separation, but no vortex | $K.C.=2.9$ Separation, but no vortex |
| V-2 | A pair of symmetric vortices | $3<K.C.<8$ | $2<K.C.<7.5$ | $4<K.C.<5$ |
| V-3 | A pair of asymmetric vortices | $8<K.C.<13$ | $7.5<K.C.<15$ | $5<K.C.<8$ Symmetry is apt to collapse |
| | | | $15<K.C.<19$ A pair of extremely asymmetric vortices | $8<K.C.<16$ |
| V-4 | The third vortex generation | $13<K.C.<20$ Weak asymmetry<br><br>$20<K.C.<26$ Intensive asymmetry | $19<K.C.$ Pseudo Karman vortex street | $16<K.C.<22$ |
| V-5 | Pseudo Karman vortex street | $26<K.C.$ | | $22<K.C.<30$ The third vortex shedding<br><br>$30<K.C.$ Pseudo Karman vortex street |

number (*Re* in abbreviation). Some delicate differences among the three studies are observed in Table 1. However, they are acceptable as inessential differences. Since it is not the purpose of this study to compare the differences among these three results, no more discussion will be mentioned here.

**(3) Experimental results and discussions**

To clarify the effect of the current on the vortex properties, the experiments were carried out under the condition that the wave height and the wave period be almost the same. Only the current velocity is varied.

Fig. 1 shows the results of experiments when the surface *K.C.* numbers $K.C._s$, which were calculated from the water particle velocity of only the wave component, are approximately equal to 3 and only the current velocity is varied. $K.C._s$ is defined as follows:
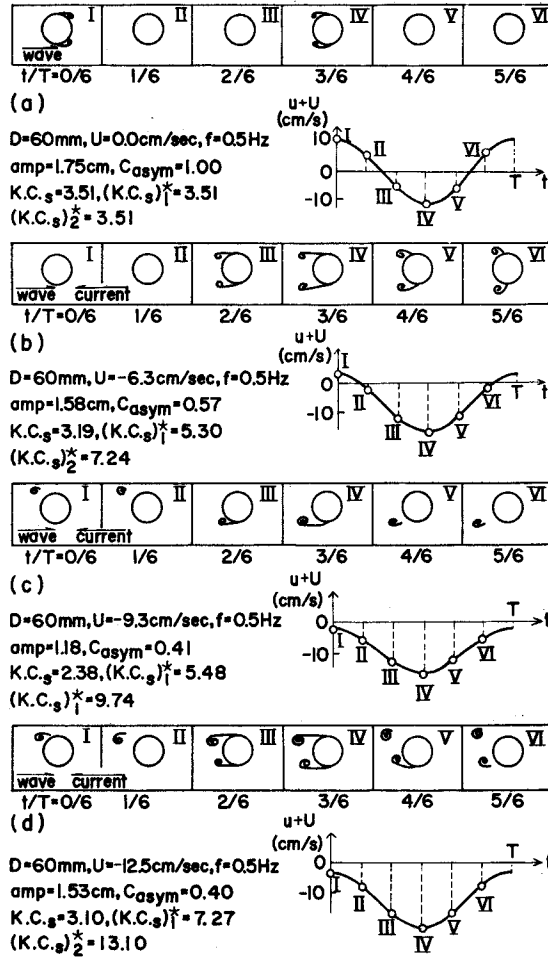
$$K.C._s = u_{ms}T/D \qquad \qquad \cdots\cdots(1)$$

Fig. 1   Changes of vortex pattern due to currents

in which, $u_{ms}$ is the velocity amplitude of the wave component at the still water level, $T$ the wave period and $D$ the diameter of a cylinder. $u_{ms}$ was calculated from the small amplitude wave theory. The subscript 's' denotes the value at the water surface. $(K.C._s)^*_1$ and $(K.C._s)^*_2$ in Fig. 1 are introduced as new $K.C.$ numbers in the co-existing field. Their definition will be described later. In these numbers, the water particle velocity is represented by a composite velocity of the wave and current component at the trough phase. The direction of the wave propagation in Fig. 1 is from left to right, and that of current is from right to left.

Fig. 1(a), which is the case of the wave-only field, shows that a pair of symmetric vorteces are generated and they are not shed from the cylinder. This vortex

pattern corresponds to V-1 in Table 1. Fig. 1(b) shows the case when a current of 6.3 cm/sec in velocity is superimposed on the waves. In this figure, it is observed that a pair of symmetric vorteces are generated at phase III, when the composite velocity becomes large, and they develop, decay and vanish as the phase proceeds. This vortex pattern at the trough phase corresponds to V-2 in Table 1, and both values of $(K.C._s)_1{}^*$ and $(K.C._s)_2{}^*$ enter into the region of the V-2 pattern.

Fig. 1(c) is the case when a faster current that in the case of (b) is superimposed, so that the movement of the water particles is uni-directional throughout the phases. It is observed that one vortex is generated in a wave period at one side, and in the following wave period one vortex is generated at the other side. It can be considered that this vortex pattern is inherent in the co-existing field which does not correspond to any pattern in the wave-only field.

As the current velocity still increases, a pair of symmetric vorteces becomes a pair of asymmetric ones as shown in Fig. 1(d). It is found that this vortex pattern corresponds to V-3 in Table 1, and both values of $(K.C._s)_1{}^*$ and $(K.C._s)_2{}^*$ enter the region of the V-3 pattern. From Fig. 1 and other visualization tests, the following vortex properties were made clear.

The vorteces which are generated at the trough phase dominate the vortex pattern all over the wave phases when the composite velocity becomes maximum. The relation between the vortex patten and $(K.C._s)_1{}^*$ or $(K.C._s)_2{}^*$ coincides with that of existing results in the wave-only field. It can not be decided here which *K.C.* number best represents the vortex properties in the co-existing field, since the experimental data are not yet sufficient. However, concerning the coefficients of the hydrodynamic force, $(K.C._s)_2{}^*$ was found to be the better parameter to describe them than $(K.C._s)_1{}^*$. Meanwhile, the flow properties during the crest phase are so affected by the still existing vorteces generated during the trough phase that the vortex properties can not be explained by the characteristics of the water particle movement.

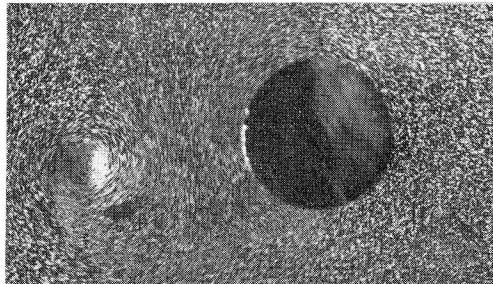The vortex properties clarified here are considered to control not only the



Photo. 1.    An example of visual observations
(this photograph corresponds to Fig. 1(c), $t/T=4/6$)

characteristics of the in-line force but also those of the lift force.  The vortex pattern shown in Fig. 1(c), for example, is different from any pattern in the wave-only field. This phenomenon makes it possible to produce an inherent property in the co-existing field, especially in the relation between the frequency of the lift force fluctuation and the wave frequency[8].

### 3.  Characteristics of in-line force acting on a circular cylinder

#### (1)  Experimental procedure

The experimental apparatus was almost same as that used in the flow visualization test.   Two vertical circular cylinders having $D=30$ mm and 60 mm diameters are mainly used in this experiment.   Test runs using a cylinder of 20 mm in diameter were added in order to obtain large $K.C.$ numbers.   The experiments were conducted under the conditions of the wave frequencies $f=0.5\sim1.6$ Hz, the wave heights $H=0\sim21.0$ cm and the velocities of the adverse currents $U=0\sim27.1$ cm/sec.   The total number of the test runs was 80 for the wave only field, and 104 for the co-existing field.   The water depth was kept constant at 40 cm.   The test cylinders were supported in a cantilever form, and the hydrodynamic forces were detected as moments by two strain gauges.

#### (2)  Procedure of analysis

The hydrodynamic forces acting on a cylinder are represented by the following Morison's equation taking into account the effect of currents:

$$dF(z)=\frac{\rho}{2}C_D(u(z)+U(z))|u(z)+U(z)|Ddz+\frac{\rho\pi}{4}C_MD^2\frac{\partial u(z)}{\partial t}dz \qquad ......( 2 )$$

in which, $dF$ is the horizontal hydrodynamic force acting on a segment $dz$, $\rho$ is the density of fluid and $C_D$ and $C_M$ are the drag and the mass coefficients respectively. The wave component in the water particle velocity $u(z)$ was assumed to be expressed by the small amplitude wave theory.   The current velocity $U(z)$ was assumed to be uniform in depth.   The hydrodynamic moments were calculated by integration from the bottom $z=-h$ to the water surface $z=\eta(t)$ by considering the arm length between the acting point of the force and the location of the strain gauges.

In this study two estimation methods of $C_D$ and $C_M$ were used.   The first one is calculated as either $C_D$ or $C_M$ at the specific phase when the inertia force or drag force becomes zero respectively.   Although this method is simple for calculating, it has some defects.   That is to say, the reliability for the calculated value decreases significantly under a certain wave and current composing ratio, because the water particle velocity or acceleration becomes nearly zero.   Furthermore, for the case when the current velocity is larger than the amplitude velocity of the wave compo-

nent, $C_M$ can not be calculated since the composite velocity never becomes zero throughout the wave phases.[9]

Therefore, it is considered that this method is applicable only for estimating $C_D$ at the trough phase when the composite velocity becomes maximum. The $C_D$ estimated by the above mentioned method is expressed as $(C_D)_{tr}$, in which the subscript 'tr' means the value at the trough phase.

A second method estimating $C_D$ and $C_M$ is that proposed by Reid[10]. By this method, water particle velocity $u$ and acceleration $\dot{u}$ are calculated from the water surface deviation $\eta$ by using a numerical filter, and $C_D$ and $C_M$ are estimated from the measured hydrodynamic force by using the least square method. The frequency response function between $\eta$ and $u$ should be used with consideration of the current. The hydrodynamic force coefficients estimated by the above method are denoted as $(C_D)_{b.f.}$ and $(C_M)_{b.f.}$, in which the subscript 'b.f.' means the best fit value.

**(3)  Predominant parameters for expressing hydrodynamic force coefficients**

Existing studies have treated the *K.C.* number and the Reynolds number as the predominant parameters expressing the hydrodynamic force coefficients. However, in the range of the Reynolds number in this experiment was between $2 \times 10^3 \sim 2 \times 10^4$, where Sarpkaya[11] reported that the changes of $C_D$ and $C_M$ with the Reynolds number are small. Accordingly, this study focuses on only the *K.C.* number as the predominant parameter on the force coefficients.

In the present study, two definitions are proposed as new *K.C.* numbers in the co-existing field. As shown in chapter 2, the vortex properties around a cylinder throughout the phases are dominated by the water particle motion around the trough phase when the composite velocity becomes maximum.

As the first *K.C.* number, considering the composite velocity at the trough phase, the following parameter is introduced:

$$(K.C.)_1{}^* = (u_m + |U|)T/D \qquad \qquad ......(3)$$

The physical meaning of the *K.C.* number can be considered as the ratio of the moving distance of a water particle in the one side direction of the cylinder $s$ to the cylinder diameter $D$.

$$K.C. = \pi s/D \qquad \qquad ......(4)$$

The second *K.C.* number is defined by the following equation expanding the above mensioned idea to the co-existing field.
For $|U| \leq u_m$

$$(K.C.)_2{}^* = 2\pi \int_{t^*}^{T/2} |U + u_m \cos \sigma t| \, dt/D \qquad \qquad ......(5)$$

in which, $t^*$ denotes the time when the composite velocity becomes zero, and

$$t^* = \cos^{-1}(-U/u_m)/\sigma \qquad \qquad \text{......(6)}$$

For $|U| > u_m$

$$(K.C.)_2{}^* = \pi UT/D \qquad \qquad \text{......(7)}$$

As an expression for the component ratio of the wave and the current, the following parameter is introduced:

$$C_{asym} = u_m/(u_m + |U|) \qquad \qquad \text{......(8)}$$

This ratio becomes 1 at the limit of wave-only and decreases to 0 as the current component becomes larger than that of the wave one. Since this parameter represents the degree of asymmetry of the flow with respect to the center of a cylinder, the subscript of 'asym' denotes the abbreviation of asymmetry.

In Eqs. (3), (5), (6) and (8), the velocity amplitude of the wave component $u_m$ is defined as the root mean square value in the range from the water surface to the bottom.

Next, the ratio of the drag force to the inertia force is discussed. The maximum values of the drag and inertia forces throughout the wave phases, $dF_{D, max}$ and $dF_{M, max}$ are expressed respectively by,

$$dF_{D, max} = (1/2)\rho C_D D(u_m + |U|)^2 dz \qquad \qquad \text{......(9)}$$

$$dF_{M, max} = (1/2)\rho\pi^2 C_M D^2(u_m/T)dz \qquad \qquad \text{......(10)}$$

Accordingly, the ratio of both forces is calculated as follows:

$$\frac{dF_{D, max}}{dF_{M, max}} = \frac{C_D}{C_M}\left(\frac{u_m T}{D}\right)\bigg/ \pi^2\left(\frac{u_m}{u_m + |U|}\right)^2 = \frac{C_D}{C_M}(K.C.)/(\pi^2 C_{asym}^2) \qquad \text{......(11)}$$

The condition that the drag force is just equal to the inertia force is examined by using Eq. (11) under the assumption that $C_D = 1$ and $C_M = 2$, independently of $K.C.$ and $C_{asym}$. The result is shown in Fig. 2, in which the predominant region of the drag or the inertia force is illustrated.
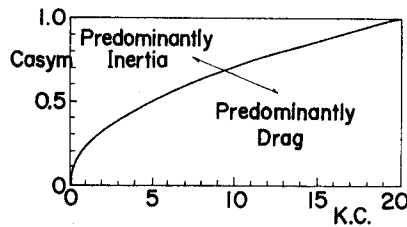


Fig. 2  Predominant region of either drag or inertia force

## (4) Experimental results and discussions

At first, experiments in the wave-only field were carried out. Figs. 3 and 4 show the relations of $C_D$ and $C_M$ with the K.C. number respectively, which were calculated from the experimental data at the specific wave phases. These results coincide well with the existing knowledge in the wave-only field.

Next, the results obtained in the co-existing field are discussed. Fig. 5 shows the relation between $(C_D)_{tr}$ calculated at the wave trough phase and the K.C. number, using the wave component only as the water particle velocity. It is observed that
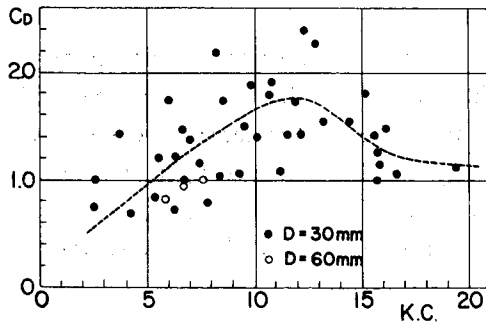
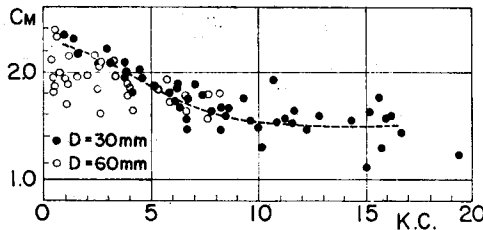Fig. 3   Drag coefficient versus K.C. number (wave-only field)

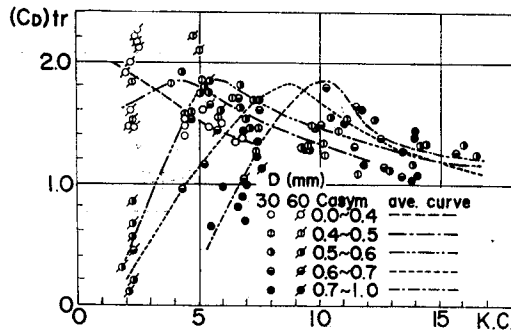Fig. 4   Mass coefficient versus K.C. number (wave-only field)

Fig. 5   Drag coefficient $(C_D)_{tr}$ at trough phase versus K.C. number
(co-existing field)

the characteristics of $(C_D)_{tr}$ are not made clear by the K.C. number only, but they become evident after classifying the data into several ranges of $C_{asym}$. Also the peaks of the averaged curves shift to the direction of an increase in the K.C. number as $C_{asym}$ increases.

The results arranged by $(K.C.)_1{}^*$ and $(K.C.)_2{}^*$, proposed as the new parameters in the co-existing field, are shown in Figs. 6 and 7, respectively. In comparing both plots, the degree of scattering in Fig. 7 using $(K.C.)_2{}^*$ is less than that in Fig. 6 using $(K.C.)_1{}^*$. In addition to this, from the view point of the physical meaning of the K.C. number, it is concluded that $(K.C.)_2{}^*$ is a more appropriate parameter than $(K.C.)_1{}^*$.

The results of $(C_D)_{b.f.}$ and $(C_M)_{b.f.}$, which are obtained by the least square method in order to best fit the calculated values with the measured ones, are discussed. Since $(K.C.)_2{}^*$ is found to be the most suitable parameter, as mentioned above, the data of $(C_D)_{b.f.}$ and $(C_M)_{b.f.}$ are also arranged by it. The results are shown in Figs. 8 and 9 respectively. Comparing Fig. 7 with Fig. 8, not much difference of the $C_D$ values by the estimating methods is found. Furthermore, from comparisons of
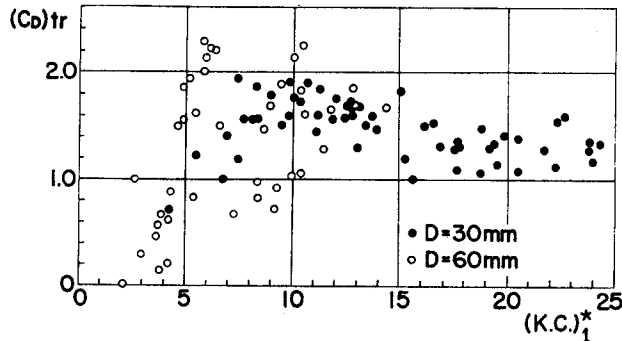


Fig. 6   Drag coefficient $(C_D)_{tr}$ at trough phase versus $(K.C.)_1{}^*$ (co-existing field)
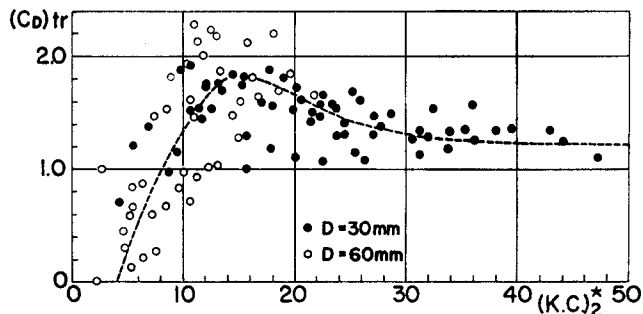


Fig. 7   Drag coefficient $(C_D)_{tr}$ at trough phase versus $(K.C.)_2{}^*$ (co-existing field)
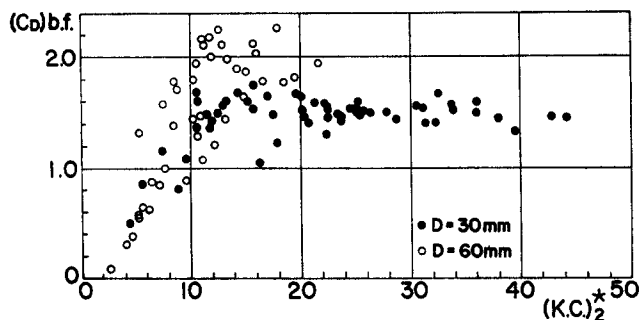
Fig. 8   Drag coefficient $(C_D)_{b.f.}$ fitting best with measured forces throughout wave phases versus $(K.C.)_2{}^*$ (co-existing field)
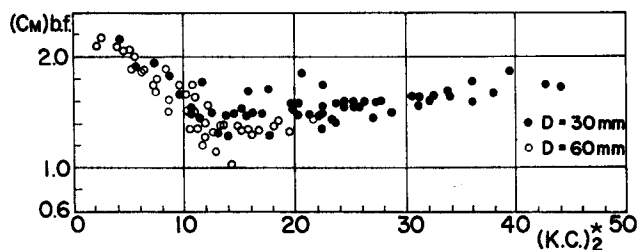


Fig. 9   Mass coefficient $(C_M)_{b.f.}$ fitting best with measured forces throughout wave phases versus $(K.C.)_2{}^*$ (co-existing field)

Figs. 7~9 and Figs. 3~4, it is confirmed that the characteristics of the hydrodynamic force coefficients in the co-existing field show a good agreement with those in the wave-only field.

The reason why the force coefficients, $C_D$ and $C_M$, are expressed well by $(K.C.)_2{}^*$, which represents the flow property around the trough phase, is considered to be because this flow property dominates the whole one throughout the wave phases.

These characteristics of $C_D$ and $C_M$ can be explained by the established physical views obtained in the wave-only field as follows.   The reason why $C_D$ becomes maximum around $(K.C.)_2{}^* = 12 \sim 15$ is because the generating vorteces in such a range of $(K.C.)_2{}^*$ are asymmetric and have a strong intensity.   The reason why $C_D$ approaches 1.2 as $(K.C.)_2{}^*$ becomes very large is because the flow property becomes similar to the steady flow.   On the other hand, the reason why $C_M$ becomes approximately 2 in the region of a small value of $(K.C.)_2{}^*$ is because the flow condition becomes close to that of the potential flow due to the small effect of viscosity.   The reason why $C_M$ becomes minimum when $C_D$ is maximum is because the inertia force apparently decreases in the treatment of Morison's equation due to residual vorteces around the cylinder.

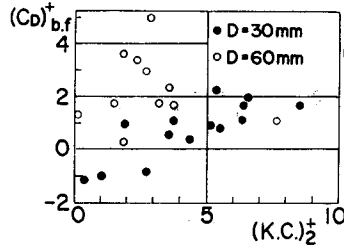In addition, several examinations were carried out as follows.   In the above

Fig. 10  Drag coefficient $(C_D)^+_{b.f.}$
fitting best during phase
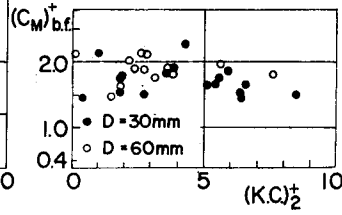of positive composite ve-
locity versus $(K.C.)_2^+$
(coexisting field)

Fig. 11  Mass coefficient $(C_M)^+_{b.f.}$
fitting best during phase
of positive composite ve-
locity versus $(K.C.)_2^+$
(coexisting field)

discussion, $C_D$ and $C_M$ were treated as being constant throughout the wave phase. However, they are considered not to be constant especially in the co-existing field, since the movement of water particles becomes asymmetric.  As a result, the flow property around the trough phase is different from that around the crest phase.  As the first examination, the hydrodynamic force coefficients, $(C_D)_{b.f.}$ and $(C_M)_{b.f.}$, were calculated separately for both phases of the trough where the moving direction of the water particles due to waves is the same as that of the current and the crest, where it is opposite to the current.  The results in the trough phase were almost same as the results in Figs. 8 and 9.  On the other hand, the results in the crest phase are plotted in Figs. 10 and 11, in which, $(K.C.)_2^+$ is the K.C. number in the crest phase calculated in the same manner as shown by Eqs. (5) and (6).  Much scattering is seen, especially in the results of $C_D$, which means that the hydrodynamic force coefficients in the crest phase can not be arranged even by the new K.C. number. This reason is because in the crest phase the effect of the residual vorteces can not be generated in the manner corresponding to the water particle movement in the region.

Next, the effect of the convective acceleration on the hydrodynamic coefficients was examined by adopting $(\partial u/\partial t + U\partial u/\partial x)$ instead of $(\partial u/\partial t)$ as the acceleration in the co-existing field.  Very little variation in the $C_D$ value was found, the difference being 0.005 at maximum.  On the other hand, the $C_M$ value using $(\partial u/\partial t + U\partial u/\partial x)$ becomes large as the current velocity is large, and it reaches 1.3 times the value using $(\partial u/\partial t)$.  However, the increase in $C_M$ is not important because in the above condition the inertia force is much smaller than the drag force.

## 4.  Conclusion

In this paper, the characteristics of the in-line hydrodynamic force in the wave

and adverse current co-existing field were discussed by clarifying the vortex properties around a circular cylinder. The main results are as follows:

(1) The vortex properties around a circular cylinder depend on the flow properties around the trough phase when the wave-current composite velocity is maximum. The vortex patterns can be classified by $(K.C.)_1^*$ or $(K.C.)_2^*$ which are introduced as new $K.C.$ numbers in the co-existing field.

(2) The results of the drag coefficient $C_D$ and the mass coefficient $C_M$ can be well arranged by $(K.C.)_2^*$, and their characteristics coincide with the existing results in the wave-only field.

(3) The relation between the vortex properties and the characteristics of the in-line hydrodynamic force in the co-existing field can be generally explained by applying the established physical view in the wave-only field.

## Acknowledgement

## References

1) Sarpkaya, T. and M. Isaacson: Mechanics of wave forces on offshore structures, Van Nostrand Reinhold Co., p. 651, 1981.

2) Verley, R.L.P. and G. Moe: The forces on a cylinder oscillating in a current, The Norwegian Institute of Technology, Report No. STF60, A79061, p. 58, 1979.

3) Horikawa, K, M. Muzuguchi, O. Kitazawa and Y. Yanagimoto: On hydrodynamic force in wave-current field (part. 1), Proc. 23th Conf. Coastal Eng. in Japan, pp. 39–44, 1976 (in Japanese).

4) Horikawa, K., O. Kitazawa, M. Nakai and M. Mizuguchi: On hydrodynamic force in wave-current field (part. 2), Proc. 24th Conf. Coastal Eng. in Japan, pp. 347–351, 1977 (in Japanese).

5) Iwagaki, Y. and H. Ishida: Flow separation, wake vorteces and pressure distribution around a circular cylinder under oscillatory waves, Proc. 15th Coastal Eng. Conf. ASCE, pp. 2341–2356, 1976.

6) Sawaragi, T. and T. Nakamura: Analytical study of wave force on a cylinder in oscillatory flow, Coastal Structures 79, Vol. 1, pp. 154–173, 1979.

7) Sawamoto, M. and K. Kikuchi: Lift forces on circular cylinder in an oscillating fluid, Proc. 26th Conf. Coastal Eng. in Japan, pp. 429–433, 1979 (in Japanese).

8) Asano, T., Y. Iwagaki and F. Nagai: On frequency locking phenomena between waves and fluctuations of lift force acting on a circular cylinder, 37th Annual Conv. of Japan Soc. of Civil Eng., Part-2, 1982 (in Japanese).

9) Asano, T., Y. Iwagaki and H. Takashina: On hydrodynamic forces acting on a vertical circular cylinder in wave-current co-existing fields, 36th Annual Conv. of Japan Soc. of Civil Eng., Part-2, pp. 783–784, 1981 (in Japanese).

10) Reid, R.O.: Correlation of water level variations with wave forces on a vertical pile for non-periodic waves, Proc. 6th Conf. Coastal Eng., pp. 749–783, 1957.

11) Sarpkaya, T.: In-line and transverse forces on cylinders in oscillatory flow at high Reynolds number, Proc. of Offshore Technology Conference, Vol. 2, pp. 95–108, 1976.